Microlensing 2000: A New Era of Microlensing Astrophysics
ASP Conference Series, Vol. 000, 2000
J.W. Menzies and P.D. Sackett, eds.

Theory of Microlensing

Andrew Gould
Dept. of Astronomy, Ohio State University, 140 W. 18th Ave., Columbus, OH, 43210-1173

Abstract.
I present a somewhat selective review of microlensing theory, covering five major areas: 1) the derivation of the basic formulae, 2) the relation between the observables and the fundamental physical parameters, 3) binaries, 4) astrometric microlensing, and 5) femtolensing.

1. Introduction

All of gravitational microlensing is reducible to a single equation, the Einstein formula for α, the deflection of light from a distant source passing by a lens of mass M at an impact parameter b,

$$\alpha = \frac{4GM}{bc^2}. \tag{1}$$

This equation has been verified experimentally by Hipparcos to an accuracy of 0.3% (Froeschle, Mignard, & Arenou 1997). Despite its apparent simplicity, equation (1) generates an incredibly rich phenomenology. The aim of this review is to present the reader with a concise introduction to microlensing phenomena from the standpoint of theory. It is impossible to cover all aspects of microlensing in the space permitted. Several good reviews of microlensing can be consulted to obtain a deeper appreciation for various aspects of the subject (Paczyński 1996; Gould 1996; Roulet & Mollerach 1997; Mao 1999b).

By definition, microlensing is gravitational lensing where the images are too close to be separately resolved. The main microlensing effect that has been discussed in the literature (and the only one that has actually been observed) is *photometric microlensing*: the magnification of the source due to the convex nature of the lens (Einstein 1936; Refsdal 1964; Paczyński 1986; Griest 1991; Nemiroff 1991). However, there are two other effects that deserve attention from the standpoint of theory: *astrometric microlensing*, the motion of the centroid of the images relative to the source, and *femtolensing*, which refers to interference effects in microlensing.

2. Observables and Physical Parameters

2.1. The Lens Diagram

Consider a lens at d_l and a more distant source at d_s that are perfectly coaligned with the observer (Fig. 1). By axial symmetry, the source is imaged into a ring

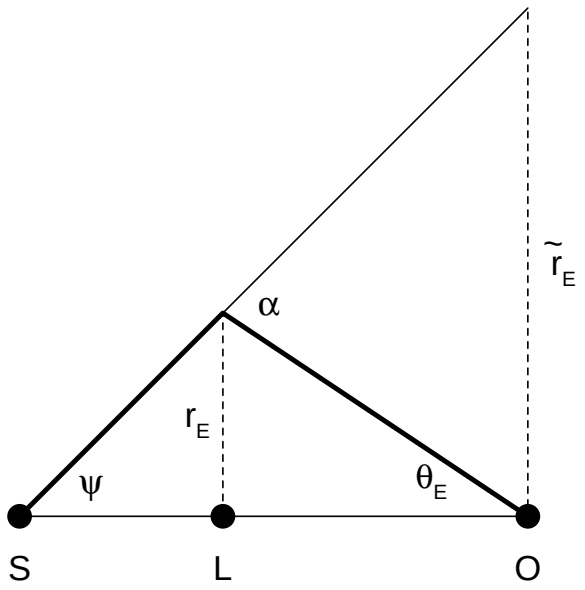

Figure 1. Basic geometry of lensing for the case when the source (S), lens (L), and observer (O), are aligned. The light is deflected by an angle α into a ring of radius $\theta_{\rm E}$. The resulting Einstein ring, $r_{\rm E}$ projected onto the observer plane is $\tilde{r}_{\rm E}$. Simple geometry relates the observables, $\theta_{\rm E}$ and $\tilde{r}_{\rm E}$ to the lens mass M and lens-source relative paralax $\pi_{\rm rel}$. See eqs. (2) and (3).

(the "Einstein ring") whose angular radius is denoted $\theta_{\rm E}$. The impact parameter, $r_{\rm E}$, is called the "physical Einstein ring", and its projection back onto the plane of the observer is called the "projected Einstein ring", $\tilde{r}_{\rm E}$. As I will show below, $\theta_{\rm E}$ and $\tilde{r}_{\rm E}$, are two of the seven observables of the system. Using the small-angle approximation, they can be related to the physical parameters, M and the source-lens relative parallax, $\pi_{\rm rel}$ (Gould 2000b). First, $\alpha/\tilde{r}_{\rm E} = \theta_{\rm E}/r_{\rm E}$, so using equation (1), one finds

$$\tilde{r}_{\rm E}\theta_{\rm E} = \alpha r_{\rm E} = \frac{4GM}{c^2}. \tag{2}$$

Second, using the exterior angle theorem, $\theta_{\rm E} = \alpha - \psi = \tilde{r}_{\rm E}/d_l - \tilde{r}_{\rm E}/d_s$, so

$$\frac{\theta_{\rm E}}{\tilde{r}_{\rm E}} = \frac{\pi_{\rm rel}}{\rm AU}. \tag{3}$$

These equations can easily be combined to yield,

$$\theta_{\rm E} = \sqrt{\frac{4GM}{c^2}\,\frac{\pi_{\rm rel}}{\rm AU}}, \qquad \tilde{r}_{\rm E} = \sqrt{\frac{4GM}{c^2}\,\frac{\rm AU}{\pi_{\rm rel}}}. \tag{4}$$

Note that if $\theta_{\rm E}$ and $\pi_{\rm rel}$ are measured in mas, $\tilde{r}_{\rm E}$ is measured in AU, and M is measured in $M_\odot/8$, then all numerical factors and physical constants in these last three equations can be ignored.

2.2. The Lensing Event

If the lens is not perfectly aligned with the source, then the axial symmetry is broken and there are only two images. A similar use of the exterior-angle theorem then yields $\theta_I^2 - \theta_I\theta_s = \theta_{\rm E}^2$, for the relation between the image positions, $\theta_{I,\pm}$ and the source position θ_s, relative to the lens. It is conventional to normalize the (vector) source position to $\theta_{\rm E}$, i.e., $\mathbf{u} \equiv \vec{\theta}_s/\theta_{\rm E}$, so that the image positions are at

$$\vec{\theta}_{I,\pm} = \pm u_\pm \hat{\mathbf{u}}, \qquad u_\pm \equiv \frac{\sqrt{u^2+4} \pm u}{2}. \tag{5}$$

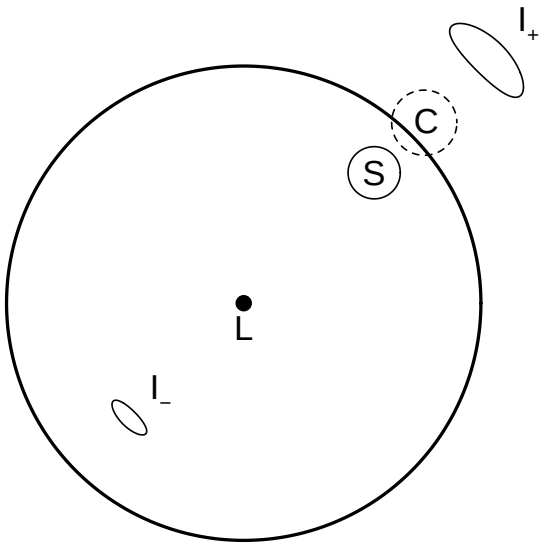

Figure 2. Source and images for a point lens. The bold line shows the Einstein ring centered on the lens (L). The two images (I_+ and I_-) of the source (S) are shown with their correct relative size and shape. The centroid of light (C) is shown at its correct position and with a size proportional to the magnification but, since the centroid is by definition unresolved, its shape is displayed arbitarily as a circle.

By Liouville's theorem, surface brightness is conserved, so for a uniformly bright source, the magnification of each of the two images $A_\pm$ is given by the ratio of the area of the image to the area of the source. See Figure 2. In the limit of a point source, this ratio reduces to the Jacobian of the transformation,

$$A_\pm = \left| \frac{\partial \vec{\theta}_{I,\pm}}{\partial \vec{\theta}_s} \right| = \frac{u_\pm^2}{u_+^2 - u_-^2}, \qquad A = A_+ + A_- = \frac{u^2+2}{u\sqrt{u^2+4}} \tag{6}$$

Since A is a monotonic function of u, the signature of a *microlensing event* is that the source becomes brighter and then fainter as the line of sight to the source gets closer to and farther from the lens. If the source, lens, and observer are all in rectilinear motion, then by the Pythagorian theorem, $u(t) = [u_0^2 + (t-t_0)^2/t_{\rm E}^2]^{1/2}$,

where t_0 is the time of closest approach, $u_0 = u(t_0)$,

$$t_{\rm E} \equiv {\theta_{\rm E}\over \mu_{\rm rel}}, \qquad \vec\mu_{\rm rel} \equiv \vec\mu_l - \vec\mu_s, \tag{7}$$

and $\vec\mu_{\rm rel}$ is the lens-source relative proper motion.

2.3. Observables

From a photometric microlensing event, one can then usually measure three parameters, t_0, u_0, and $t_{\rm E}$. Of these, the first two tell us nothing about the lens, and the third is related to M, $\pi_{\rm rel}$, and $\mu_{\rm rel}$ in a complicated way through equations (4) and (7). However, as mentioned above, there are actually seven (scalar) quantities that can in principle be observed in a microlensing event. These are: $t_{\rm E}$, $\theta_{\rm E}$, $\tilde r_{\rm E}$, ϕ (the angle of lens-source relative proper motion), and the source parallax and proper motion, π_s, and $\vec\mu_s$, which can be measured astrometrically after the event.

To date, there have been only a handful of measurements of $\theta_{\rm E}$, $\tilde r_{\rm E}$, and ϕ, no measurements of $\vec\mu_s$, and only estimates of π_s (although these are probably very good). However, all that could radically change in the next decade. I first discuss what it means that these quantities are "observable" and then briefly outline future prospects.

The angular Einstein ring $\theta_{\rm E}$ can be measured by scaling the event against some known "angular ruler" on the sky. The only such "ruler" to be used to date is the angular size of the source (Gould 1994a; Nemiroff & Wickramasinghe 1994; Witt & Mao 1994), which can be determined from the source flux and color, together with the empirical color/surface-brightness relation (van Belle 1999; Albrow et al. 2000a). So far, $\theta_{\rm E}$ has been measured for only 7 of the ~ 500 events detected to date (Alcock et al. 1997,2000; Albrow et al. 1999a,2000a; Afonso et al. 2000). Many other methods have been proposed (see Gould 1996 for a review; Han & Gould 1997), but none have been carried out.

The projected Einstein ring $\tilde r_{\rm E}$ can be measured by scaling the event against some known "physical ruler" in the plane of the observer. Three such "rulers" have been proposed, but the only one to be used to date is the Earth's orbit which induces a wobble in the light curve (Gould 1992b). Because this wobble depends on the Earth's motion being non-rectilinear, it is only significant if the event lasts more than a radian (i.e., $t_{\rm E} \gtrsim 58\,{\rm days}$), and such events are very rare. To date, only about a half dozen events have measured $\tilde r_{\rm E}$ (Alcock et al. 1995; Bennett et al. 1997; Mao 1999a). Another approach is to observe the event simultaneously from two locations ("parallax"). Since $\tilde r_{\rm E} \sim 5\,{\rm AU}$, it would be best if the second location were in solar orbit (Refsdal 1966; Gould 1994b).

The essential idea of a parallax satellite is illustrated in Figure 5 of Gould (1996). Basically, the Earth and the satellite each see a different microlensing event characterized respectively by $(t_{0,\oplus}, u_{0,\oplus}, t_{{\rm E},\oplus})$, and $(t_{0,{\rm sat}}, u_{0,{\rm sat}}, t_{{\rm E},{\rm sat}})$. To zeroth order $t_{{\rm E},{\rm sat}} \simeq t_{{\rm E},\oplus}$, but the differences in the other two components,

$$\Delta{\bf u} \equiv (\Delta t_0/t_{\rm E}, \Delta u_0) = (t_{0,{\rm sat}}/t_{\rm E}, u_{0,{\rm sat}}) - (t_{0,\oplus}/t_{\rm E}, u_{0,\oplus}), \tag{8}$$

give the displacement in the Einstein ring of the satellite relative to the Earth. That is,

$$\tilde r_{\rm E} = {d_{\rm sat}\over \Delta u}, \tag{9}$$

where $d_{\rm sat}$ is the Earth-satellite separation (projected onto the plane perpendicular to the line of sight). There is actually a four-fold ambiguity in $\Delta u_0 = \pm(u_{0,\rm sat} \pm u_{0,\oplus})$ but this can be resolved, at least in principle, from the small difference in Einstein timescales which constrains Δu_0 by (Gould 1995),

$$w_\perp \Delta u_0 + w_\parallel \frac{\Delta t_{\rm E}}{t_{\rm E}} + d_{\rm sat} \frac{\Delta t_{\rm E}}{t_{\rm E}^2} = 0, \tag{10}$$

where $w_\parallel$ and $w_\perp$ are the components of the Earth-satellite relative velocity respectively parallel and perperdicular to the Earth-satellite separation vector. Boutreux & Gould (1996) and Gaudi & Gould (1997) showed that the degency could be broken with relatively modest satellite parameters. Unfortunately, no such satellite has been launched.

In a few specialized situations, it should be possible to obtain parallaxes using Earth-sized baselines (Hardy & Walker 1995; Holz & Wald 1996; Gould 1997; Gould & Andronov 1999; Honma 1999), but to date no such measurements have been made. All measurements of $\tilde{r}_{\rm E}$ simultaneously measure ϕ, and to date no other measurements of ϕ have been made.

2.4. Physical Parameters in Terms of Observables

It is convenient to replace $t_{\rm E}$ and ϕ together by $\vec{\mu}_{\rm E}$ whose direction is ϕ and whose magnitude is $\mu_{\rm E} \equiv t_{\rm E}^{-1}$, and to replace $\tilde{r}_{\rm E}$ by $\pi_{\rm E} \equiv {\rm AU}/\tilde{r}_{\rm E}$. Then equation (4) can be rewritten as,

$$\theta_{\rm E} = \sqrt{\kappa M \pi_{\rm rel}}, \qquad \pi_{\rm E} = \sqrt{\frac{\pi_{\rm rel}}{\kappa M}}, \qquad \kappa \equiv \frac{4G}{c^2\,{\rm AU}} \simeq 8.144\,\frac{\rm mas}{M_\odot}, \tag{11}$$

and the physical parameters can be written in terms of the observables as,

$$M = \frac{\theta_{\rm E}}{\kappa \pi_{\rm E}}, \qquad \pi_l = \pi_{\rm E}\theta_{\rm E} + \pi_s, \qquad \vec{\mu}_l = \vec{\mu}_{\rm E}\theta_{\rm E} + \vec{\mu}_s. \tag{12}$$

3. Astrometric Microlensing

While microlensing images cannot be resolved, the centroid of the images deviates from the source position by

$$\delta\vec{\theta} = \frac{A_+\vec{\theta}_{I,+} + A_-\vec{\theta}_{I,-}}{A_+ + A_-} - \vec{\theta}_s = \frac{\mathbf{u}}{u^2+2}\theta_{\rm E}, \tag{13}$$

which reaches a maximum of $\theta_{\rm E}/\sqrt{8}$ when $u = \sqrt{2}$. See Figure 1. Since typically $\theta_{\rm E} \sim 300\mu$as, $\delta\vec{\theta}$ is well within the range of detection of the Space Interferometry Mission (SIM) and perhaps ground-based interferometers as well. While it is not obvious from equation (13), if $\mathbf{u}(t)$ is rectilinear, then $\delta\vec{\theta}$ traces out an ellipse. The size of the ellipse gives $\theta_{\rm E}$ and its orientation gives ϕ. Hence, if microlensing were monitored astrometrically, it would be possible to *routinely* recover these two parameters (Boden, Shao, & Van Buren 1998; Paczyński 1998). In fact, astrometric microlensing has a host of other potential applications including measurement of the lens brightness (Jeong, Han, & Park 1999; Han &

Jeong 1999), removal of degeneracies due to blended light from unmicrolensed sources (Han & Kim 1999), and the detection and characterization of planetary (Safizadeh, Dalal & Griest 1999) and binary microlenses (Chang & Han 1999; Han, Chun, & Chang 1999).

Because at late times the astrometric signature falls off as u^{-1} (eq. 13), compared to u^{-4} for the photometric signature (eq. 6), it could in principle be possible to measure $\tilde{r}_{\rm E}$ astrometrically from the Earth's orbital motion, even for events with $t_{\rm E} \ll 58\,{\rm days}$ (Boden et al. 1998; Paczyński 1998). If practical, this would mean that all the observables listed in § 2.3 could be extracted from astrometric observations alone. Unfortunately, such measurements are not practical (Gould & Salim 1999).

Nevertheless, using SIM one can in fact extract all seven parameters, and therefore can accurately determine both the masses and distances of the lenses. SIM makes its astrometric measurements by centroiding the fringe, i.e., by *counting photons* as a function of fringe position. This means that SIM's *astrometric* measurements are simultaneously *photometric* measurements. Since SIM will be launched into solar orbit, it therefore can effectively act as a parallax satellite (Gould & Salim 1999). Moreover, SIM can break the degeneracy in Δu_0 in two ways: photometrically (according to eq. 10) and astrometrically (by measuring the angle ϕ associated with the astrometric ellipse, eq. 13).

An alternate approach to measuring $\tilde{r}_{\rm E}$ would be to compare SIM and ground-based *astrometry* rather than *photometry* (Han & Kim 2000).

Another important application of astrometric micolensing is to measure the masses of nearby stars (Refsdal 1964; Paczyński 1995, 1998; Miralda-Escudé 1996). Equation (13) still effectively describes the astrometric deflection, but since typically $u \gg 1$, this equation can be more simply written as

$$\Delta\theta = \frac{\kappa M \pi_{\rm rel}}{\theta_{\rm rel}}, \tag{14}$$

where $\theta_{\rm rel} \equiv |\vec{\theta}_l - \vec{\theta}_s|$. In this form, it is clear that the probability that a given lens will come close enough to a background source to allow a mass measurement of fixed precision in a fixed amount of time is

$$P \propto M \pi_l \mu_l N, \tag{15}$$

where N is the density of background sources (Gould 2000a). Hence, the best place to look for such candidates is a proper-motion selected catalog near the Galactic plane. In fact, the selection of such candidates is a complex undertaking, but good progress is being made (Salim & Gould 2000).

4. Binary Lenses

Binary microlensing is one of the most active fields of theoretical investigation in microlensing today. In part this is due to the mathematical complexity of the subject and in part to the demands that are being placed on theory by new, very precise observations of binary events. Schneider & Weiss (1986) made a careful early study of binary lenses despite the fact that they never expected any to be detected (P. Schneider 1994, private communication), in order to

learn about caustics in quasar macrolensing. Indeed caustics are the main new features of binaries relative to point lenses. These are closed curves in the source plane where a point source is infinitely magnified. The curves are composed of 3 or more concave segments that meet at cusps. Binary lenses can have 1, 2, or 3 closed caustic curves. If the two masses are separated by approximately an Einstein radius, then there is a single 6-cusp caustic. If they are separated by much more than an Einstein ring, then there are two 4-cusp caustics, one associated with each member of the binary. If the masses are much closer than an Einstein ring, there is a central 4-cusp caustic and two outlying 3-cusp caustics. Figure 3 shows two cases of the 6-cusp caustic, one close to breaking up into the two caustics characteristic of a wide binary and the other close breaking up into the three caustics characteristic of a close binary. Witt (1990) developed a simple algorithm for finding these caustics. Multiple-lens systems can have even more complicated caustic structures (Rhie 1997; Gaudi, Naber, & Sackett 1998).

4.1. Binary Lens Parameters

Recall that a point-lens light curve is defined by just three parameters, t_0, u_0, and $t_{\rm E}$. These three generalize to the case of binaries as follows: u_0 is now the smallest separation of the source relative to the center of mass (alternatively geometric center) of the binary, t_0 is the time when $u = u_0$, and $t_{\rm E}$ is the timescale associated with the combined mass of the binary. At least three additional parameters are required to describe a binary lens: the angle α at which the source crosses the binary axis, the binary mass ratio q, and the projected separation of the binary in units of the Einstein ring. Several additional parameters may be required in particular cases. If caustic crossings are observed, then the infinite magnification of the caustic is smeared out by the finite size of the source, so one must specify $\rho_* = \theta_*/\theta_{\rm E}$, where θ_* is the angular size of the source. If the observations of the crossing are sufficiently precise, one must specify one or more limb-darkening coefficients for each band of observation (Albrow et al. 1999a, 2000a; Afonso et al. 2000). Finally, it is possible that the binary's rotation is detectable in which case one or more parameters are required to describe that (Dominik 1998a; Albrow et al. 2000a). In addition, binary light curves often have data from several observatories in which case one needs two parameters (source flux and background flux) for each observatory.

4.2. Binary Lens Lightcurve Fitting

The problem of fitting binary-lens lightcurves is extremely complicated and is still very much under active investigation. There are actually three inter-related difficulties. First, as discussed in § 4.1, the parameter space is large. Second, it turns out the minima of χ^2 over this space are not well behaved. Third, the evaluation of the magnification for a finite source straddling or near a caustic can be computationally time consuming. The combination of these three factors means that a brute force search for solutions can well fail or, worse yet, settle on a false minimum.

The ideas for tackling these problems go back to the detection of the first binary microlens OGLE-7 (Udalski et al. 1994). There are two major categories: ideas for improving efficiency in the evaluation of the magnification, and ideas

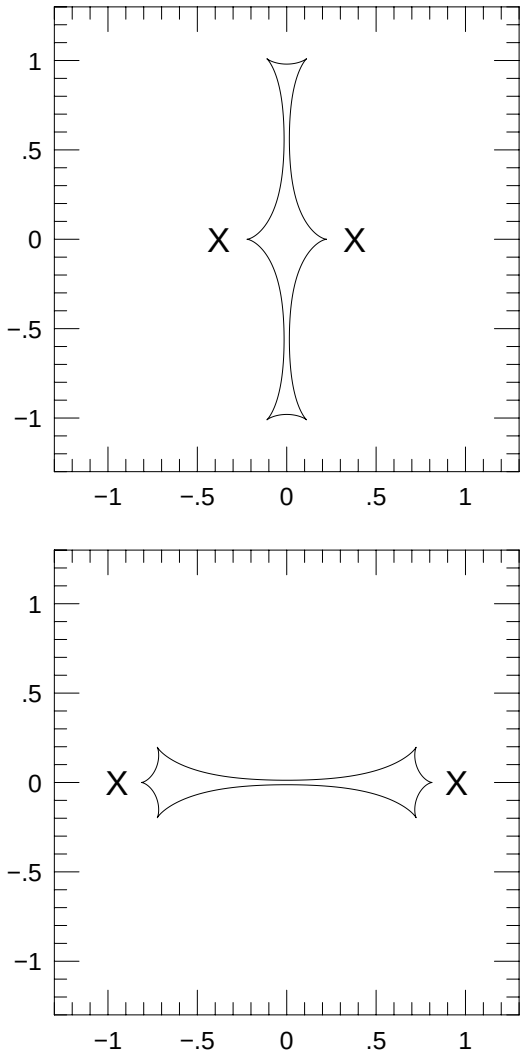

Figure 3. Two extreme examples of 6-cusp caustics generated by equal mass binaries. The tick marks are in units of Einstein radii. In each case, the crosses show the positions of the two components. The upper panel shows a relatively close binary with the components separated by $d = 0.76$ Einstein radii. For $d < 2^{-1/2}$ the caustic would break up into three caustics, a central 4-cusp caustic plus two outlying 3-cusp caustics. The lower panel shows a relatively wide binary with $d = 1.9$. For $d > 2$ the caustic would break up into two 4-cusp caustics.

for cutting down the region of parameter space that must be searched. For the first, various methods have been developed by Kayser & Schramm (1988), Bennett & Rhie (1996), Gould & Gaucherel (1997), Wambsganss (1997) and Dominik (1998b), although in fact all are still fairly time consuming. For the second, Mao & Di Stefano (1995) developed a densely sampled library of point-source binary microlensing events, each of which is characterized by cataloged "features" such as the number of maxima, heights of peaks, etc. They can then examine individual events, characterize their "features," and search their library for events that are consistent with these features. Di Stefano & Perna (1997) suggested that binary lenses could be fitted by decomposing the observed light curve into a linear combination of basis functions. The coefficients of these functions could then be compared to those fitted to a library of events in order to isolate viable regions of parameter space. This is essentially the same method as Mao & Di Stefano (1995), except that, rather than use gross features to identify similar light curves, one uses the coefficients of the polynomial expansion, which is more quantitative and presumably more robust.

Albrow et al. (1999b) developed a hybrid approach that both simplifies the search of parameter space and vastly reduces the computation time for individual light curves. It makes use of the fact that one of the very few things that is simple about a binary microlens is the behavior of its magnification very near to a caustic. A source inside a caustic will be imaged into five images, while outside the caustics it will be imaged into three images. Hence, at the caustic two images appear or disappear. These images are infinitely magnified. In the immediate neighborhood of a caustic (assuming one is not near a cusp), the magnification of the two new images diverges as $A_2 \propto (-\Delta u_\perp)^{-1/2}$, where $\Delta u_\perp$ is the perpendicular separation of the source from the caustic (in units of $\theta_{\rm E}$). On the other hand, the three other images are unaffected by the approach of the caustic, so $A_3 \sim$const. Hence, the total magnification is given by (Schneider & Weiss 1987)

$$A = A_2 + A_3 \simeq \left(-\frac{\Delta u_\perp}{u_r}\right)^{-1/2} \Theta(-\Delta u_\perp) + A_{cc}, \tag{16}$$

where u_r is a constant that characterizes the approach to the caustic, A_{cc} is the magnification just outside the caustic crossing, and Θ is a step function. For a source of uniform brightness, or limb darkened in some specified way, one can therefore write a relatively simple expression for the total magnification as a function $\Delta u_\perp$ (Albrow et al. 1999b; Afonso et al. 2000).

4.3. Degeneracies

By fitting just the caustic-crossing data to a simple form based on equation (16), Albrow et al. (1999b) were able to reduce the search space from 7 to 5 dimensions and so effect a brute force search. This turned up a degeneracy between a wide-binary geometry and a close-binary geometry that both equally well accounted for the observed light curve. The Albrow et al. (1999b) data did not cover large parts of the light curve, but even when Afonso et al. (2000) combined these data with very extensive data sets from four other microlensing collaborations, the close/wide degeneracy survived. Simultaneously, Dominik (1999b) discovered a

whole class of close/wide binary degeneracies whose roots lie deep in the lens equation itself.

This was unexpected. It was previously known that various observed light curves could be fit by several radically different binary geometries (Dominik 1999a). However, Han et al. (1999) showed that these geometries produced radically different astrometric deviations, so that the photometric degeneracy could be taken to be in some sense "accidental". Moreover, for all of the examples examined by Dominik (1999a) and Han et al. (1999), the data, while reasonably good, were substantially poorer in quality than those used by Afonso et al. (2000). Hence, it was plausible to hope that with better photometric data, the degeneracies could be resolved. However, since the Dominik (1999b) degeneracies are rooted in the lens equation, they may prove more intractible. For example, Gould & Han (2000) showed that, in contrast to the cases examined by Han et al. (1999), the wide and close models presented by Afonso et al. (2000) generated similar astrometric deviations, although they could be distinguished with sufficiently late time data. On the other hand, Albrow et al. (2000b) showed that in at least one case this degeneracy is easily broken with photometric data alone.

5. Femtolensing

Femtolensing refers to interference effects in microlensing and derives its name from the very small angular scales that are usually required to produce such effects (Gould 1992a). To date, work on femtolensing has been almost entirely theoretical, although there has been at least one significant observational result.

As I mentioned in § 2.2, the magnification is given by the ratio of the area of the image to the area of the source, but this applies only to single images. Multiple images will in general interfere with one another. The reason that this can generally be ignored (and so one can write $A = A_+ + A_-$ as I did in eq. 6) is that usually the source is large enough that for some parts the two images interfere constructively, and for other parts they do so destructively, so that one can simply add intensities rather than amplitudes.

The validity of this approximation then depends on how rapidly the relative phase (proportional to the time delay) varies across the source. For a point lens and for $u \ll 1$, the time delay between the images is given by $\Delta t = 8GM/c^3(1+z_L)u$ where z_L is the redshift of the lens. The phase delay is therefore,

$$\Delta\phi = \frac{E\Delta t}{h} = 9.5\times 10^9 \frac{M}{M_\odot}\,\frac{E}{\rm eV}\,(1+z_L)u, \tag{17}$$

where E is the energy of the photon. Hence, for ordinary Galactic microlensing observed in optical light, the interference effects are completely wiped out unless the source covers only a tiny part of the Einstein ring, $\rho_* \lesssim 10^{-10}$. Thus, applications of femtolensing require a search for unusual regions of parameter space. However, if such regions of parameter space can be identified, the effects can be dramatic: if the magnifications of the images are written in terms of $u_\pm$ (eq. 6), it is not difficult to show that,

$$\mathcal{A}_\pm = (A_+^{1/2} \pm A_-^{1/2})^2 = (1+4/u^2)^{\pm 1/2}, \tag{18}$$

where $\mathcal{A}_\pm$ are the magnifications at constructive and destructive interference. Hence the ratio of the peaks to the troughs is $\mathcal{A}_+/\mathcal{A}_- = (1 + 4/u^2)$, which for typical $u \sim 0.5$ can be quite large. Hence, the interference pattern should manifest itself regardless of what intrinsic spectral features the source has.

Femtolensing was first discussed by Mandzhos (1981) and further work was done by Schneider & Schmidt-Burgk (1985) and Deguchi & Watson (1986). Peterson & Falk (1991) were the first to confront the problem of scales posed by equation (17). They considered radio sources (and so gained about 5 orders of magnitude relative to the optical) and advocated high signal-to-noise ratio observations that could detect the O(1/N) effects if the source subtends N fringes.

Gould (1992a) sought to overcome the huge factor in equation (17) by going to smaller M. He showed that asteroid-sized objects ($M \sim 10^{-16}\,M_\odot$) could femtolens gamma-ray bursts (i.e., $E \sim$ MeV). Plugging these numbers into equation (17) yields phase changes $\Delta\phi \sim 1$ over the entire Einstein ring. This is the only femtolensing suggestion that has ever been carried out in practice: Marani et al. (1999) searched BATSE and Ulysses data for femtolensing (as well as several other types of lensing) and used their null results to place weak limits on cosmological lenses in this mass regime. Kolb & Tkachev (1996) showed that these type of observations can also be used to probe for axion clusters to determine if such axions make up the dark matter.

Ulmer & Goodman (1995) developed a formalism capable of going beyond the semi-classical approximation of previous investigations. They thereby found effects that are in principle observable even at optical wavelegths and solar masses, despite the seemingly pessimistic implications of equation (17). Jaroszynski, & Paczyński (1995) then showed that these results could have implications for microlensing observations of Huchra's Lens.

I close this review with a description of another potential application of femtolensing due to Gould & Gaudi (1997). The Einstein ring associated with a typical M star at $\sim 20\,$pc is $\theta_{\rm E} \sim 10\,$mas, corresponding to $r_{\rm E} \sim 0.2\,$AU. Hence, the binary companions of such stars are likely to be several orders of magnitude farther away. The binary lens can then be approximated as a point lens perturbed by a weak shear due to the companion. This produces a Chang-Refsdal lens (Chang & Refsdal 1979, 1984), which is more thoroughly described by Schneider, Ehlers, & Falco (1992). A source lying inside the caustic and near one of the cusps will produce four images near the Einstein ring, three highly magnified images on the same side of the Einstein ring and one moderately magnified image (which we will henceforth ignore) on the other. Depending on the details of the geometry, the three images can easily be magnified 10^6 times in one direction but are not much affected (indeed shrunk by a factor 2) in the other. Thus a $10^8\,M_\odot$ black hole (Schwarzschild radius 2 AU) at the center of a quasar at 1 Gpc, could be magnified in one direction from 2 nas, to 2 mas, and so could easily be resolved with a space-based optical interferometer having a baseline of a few hundred meters.

The only problem, then, is how to get similar resolution in the other direction. Femtolensing provides the answer. Because the three images are not magnified in the direction perpendicular to the Einstein ring, they will each necessarily contain images not only of the black hole, but of considerable other junk along one-dimensional bands cutting through its neighborhood. The three bands

from the three images will cut accross one another and will only intersect along a length approximately equal to the width of the bands, i.e., $\sim 1\,$AU. If light from two of these images is brought together and dispersed in a spectrograph, then only the light from the intersecting region will give rise to interference fringes. The amplitude of these fringes will be set by the ratio of the length in the source plane over which the time delay between the images differs by 1 wavelength to the width of the bands. For typical parameters this could be a few percent. Since the $V \sim 22$ quasar will be magnified $\sim 10^6$ times to $V \sim 7$, this should not be difficult to detect.

There are a few difficulties that must be overcome to make this work in practice. First, the nearest position from which a dwarf star appears aligned with a quasar lies about 40 AU from the Sun. So while the huge "primary" of this "femtolens telescope" (the dwarf star) comes for free, getting the "secondary optics" aligned with the primary is a big job. Second, unlike other space missions that deliver payloads to 40 AU (e.g., the Voyagers), this package must be stopped at 40 AU so that it remains aligned with the dwarf star and quasar. Third, there are station keeping problems because the telescope will gradually fall out of alignment due to the Sun's gravity and will have to be realigned about every 10 hours. However, what sort of theorist would recoil from a few engineering challenges?

6. Conclusion

When microlensing experiments began in the early 1990s, few participants expected that there was much room for theoretical development at all. The physical effect (eq. 1) was completely understood, and the basic equations of microlensing had all been worked out. A decade later, microlensing theory has shown itself to be a very dynamic field. The original problems turned out to be much richer than expected, while new observations and new developments in instrumention have raised new problems. Thus, microlensing theory promises to remain vibrant.

Acknowledgements: This work was supported by grant AST 97-27520 from the NSF.

References

Afonso, C. et al. 2000, ApJ, 532, 000 (astro-ph/9907247)
Albrow, M. et al. 1999a, ApJ, 522, 1011
Albrow, M. et al. 1999b, ApJ, 522, 1022
Albrow, M. et al. 2000a, ApJ, 534, 000 (astro-ph/9910307)
Albrow, M. et al. 2000b, in preparation
Alcock, C., et al. 1995 ApJ, 454, L125
Alcock, C., et al. 1997 ApJ, 491, 436
Alcock, C., et al. 2000 ApJ, submitted (astro-ph/9907369)
Bennett, D.B. 1997, BAAS, 191, 8303
Bennett, D.P. & Rhie S.H. 1996, ApJ, 472, 660

Boden, A.F., Shao, M., & Van Buren, D. 1998 ApJ, 502, 538
Boutreux, T., & Gould, A. 1996, ApJ, 462, 705
Chang, K. & Han, C. 1999, ApJ, 525, 434 (astro-ph/00011930)
Chang, K. & Refsdal, S. 1979, Nature, 282, 561
Chang, K. & Refsdal, S. 1984, A&A, 130, 157
Deguchi, S., & Watson, W.D. 1986, ApJ, 307, 30
Di Stefano, R., & Perna, R. 1997, ApJ, 488, 55
Dominik, M. 1998a, A&A, 329, 361
Dominik, M. 1998b, A&A, 333, L79
Dominik, M. 1999a, A&A, 341, 943
Dominik, M. 1999b, A&A, 349, 108
Einstein, A. 1936, Science, 84, 506
Froeschle, M., Mignard, F., & Arenou, F. 1997, Proceedings of the ESA Symposium 'Hipparcos – Venice '97', p. 49, ESA SP-402
Gaudi, B.S., & Gould, A. 1997, 477, 152
Gaudi, B.S., Naber, R.M., & Sackett, P.D. 1998, 502, L33
Gould, A. 1992a, ApJ, 386, L5
Gould, A. 1992b, ApJ, 392, 442
Gould, A. 1994a, ApJ, 421, L71
Gould, A. 1994b, ApJ, 421, L75
Gould, A. 1995, ApJ, 441, L21
Gould, A. 1996, PASP, 108, 465
Gould, A. 1997, ApJ, 480, 188
Gould, A. 2000a, ApJ, submitted (astro-ph/9909455)
Gould, A. 2000b, ApJ, submitted (astro-ph/0001421)
Gould, A. & Andronov, N. 1999, ApJ, 516, 236
Gould, A. & Gaucherel, C. 1997, ApJ, 477, 580
Gould, A. & Gaudi, B.S. 1997, ApJ, 486, 687
Gould, A. & Han, C. 2000, ApJ, 538, 000 (astro-ph/00011930)
Gould, A., & Salim, S. 1999, ApJ, 524, 794
Griest, K. 1991, ApJ, 366, 412
Han, C., Chun, M.S., & Chang, K. 1999, 526, 405
Han, C., & Gould, A. 1997, ApJ, 480, 196
Han, C., & Jeong, Y. 1999, MNRAS, 309, 404
Han, C., & Kim, H.-I. 2000, ApJ, 528, 687
Han, C., & Kim, T.-W. 1999, MNRAS, 305, 795
Hardy, S.J., & Walker, M.A. 1995, MNRAS, 276, L79
Holz, D.E., & Wald, R.M. 1996, ApJ, 471, 64
Honma, M. 1999, ApJ, 517, L35
Jaroszynski, M., & Paczyński, B. 1995, ApJ, 455, 433
Jeong, Y., Han, C., & Park, S.H. 1999, MNRAS, 304, 845

Kayser, R., & Schramm, T. 1998, A&A, 191, 39

Kolb, E.W., & Tkachev, I.I. 1996, ApJ, 460, L25

Mandzhos, A.V. 1981, Soviet Ast., 7, L213

Mao, S. 1999a, A&A, 350, L19

Mao, S. 1999b, in Gravitational Lensing, Recent Progress and Future Goals, Boston University, July 1999, ed. T.G. Brainerd and C.S. Kochanek, in press (astro-ph/9909302)

Mao, S., & Di Stefano, R. 1995, ApJ, 440 22

Marani, G.F., Nemiroff, R.J., Norris, J.P., Hurley, K., & Bonnell, J.T., 1999, ApJ512, L13

Miralda-Escudé, J. 1996, ApJ, 470, L113

Nemiroff, R.J. 1991, A&A, 247, 73

Nemiroff, R.J. & Wickramasinghe, W.A.D.T. 1994, ApJ, 424, L21

Paczyński, B. 1986, ApJ, 304, 1

Paczyński, B. 1995, Acta Astron., 45, 345

Paczyński, B. 1996, ARA&A, 34, 419

Paczyński, B. 1998, ApJ, 494, L23

Peterson, J.B., & Falk, T. 1991, ApJ, 374, L5

Refsdal, S. 1964, MNRAS, 128, 295

Refsdal, S. 1966, MNRAS, 134, 315

Rhie, S.H. 1997, ApJ, 484, 63

Roulet, E., & Mollerach, S. 1997, Physics Reports, 279, 68

Safizadeh, N., Dalal, N., & Griest, K. 1999, ApJ, 522, 512

Salim, S., & Gould, A., 2000 ApJ, 539, 000

Schneider, P., Ehlers, J., & Falco, E.E. 1992, Gravitational Lenses (Berlin: Springer)

Schneider, P., & Schmidt-Burgk, J. 1985, A&A, 148, 369

Schneider, P., & Weiss, A. 1986, A&A, 164, 237

Schneider, P., & Weiss, A. 1987, A&A, 171, 49

Udalski, A., Szymański, M., Pietrzyński, G., Kubiak, M., Woźniak, P., & Żebruń, K. 1998, Acta Astron., 48, 431

Ulmer, A., & Goodman, J. 1995, ApJ442, 67

van Belle, G.T. 1999, PASP, 111, 1515

Wambsganss, J. 1997, MNRAS, 284, 172

Witt, H.J. 1990, A&A, 236, 311

Witt, H.J. & Mao, S. 1994, ApJ, 429, 66